ELSEVIER

Journal of Organometallic Chemistry 529 (1997) 35–50

Journal of Organometallic Chemistry

Conformational diastereoisomerism in *tris*-(2-alkylimino) triphenylphosphines

Mark R. Whitnall [a], King Kuok (Mimi) Hii [b], Mark Thornton-Pett [a], Terence P. Kee [a,*]

[a] *School of Chemistry, University of Leeds, Woodhouse Lane, Leeds LS2 9JT, UK*
[b] *Dyson Perrins Laboratory, South Parks Road, Oxford OX1 3QY, UK*

Received 31 May 1996; revised 13 September 1996

Abstract

A combination of one-dimensional, two-dimensional and nuclear Overhauser experiments allow complete NMR spectroscopic characterisation of the trifunctionalised triphenylphosphine, *tris*-(2-carboxaldehyde)triphenylphosphine **1**. A single-crystal X-ray diffraction study reveals the expected canted C_3-conformation of the phenyl rings with each of the carboxaldehyde groups occupying sterically more favoured *exo* positions. Two of the carboxaldehyde functions adopt *cis* conformations (oxygen atom directed towards phosphorus) whilst the third displays the *trans* conformation, an arrangement which we believe is connected with the adoption of hydrogen-bonded dimers in the crystal lattice. Variable temperature ^{1}H NMR investigations on the trifunctionalised organophosphorus compound *tris*-(2-n-propylimino)triphenylphosphine **5** suggest the freezing out of a low temperature conformation lacking planar symmetry below ca. 240 K. Epimerization of this dynamic conformational equilibrium is possible upon replacing the n-propyl function with an enantiomerically pure substituent. Thus the enantiomerically pure *tris*-functionalised compound *tris*-{2-[(*S*)-α-methylbenzylimino]}triphenylphosphine **6**, prepared by condensation of *tris*-(2-carboxaldehyde)triphenylphosphine with (*S*)-α-methylbenzylamine, undergoes a dynamic equilibrium between diastereoisomeric conformations, each with local C_3-symmetry at the phosphorus atom. An energy barrier E_a of 50(2) kJ mol^{-1} has been determined for this process with $\Delta H^{\ddagger}$ of 48(2) kJ mol^{-1} and $\Delta S^{\ddagger}$ of $-25(2)$ J K^{-1} mol^{-1}. The low diastereoselectivity between chiral conformations of 6% translates to an equilibrium constant K of 0.89 (at 243 K) with $\Delta G_{eq} = 236(3)$ J mol^{-1}, suggesting very little energy difference between epimers under these conditions. We speculate that one reason for low diastereoselectivity is that the O-*trans-exo* carboxaldehyde conformation is favoured over the O-*cis-exo* form and that in the former, intramolecular interactions between chiral substituents, and hence propeller conformational preferences, are minimised.

Keywords: Conformation; Functionalised triphenylphosphines; Dynamics; Helical chirality

1. Introduction

The field of phospho-transfer (PT) chemistry, the chemical transfer of phosphorus-containing groups from one site to another or the transfer of stereoelectronic information via a phosphorus-containing function, is an extremely versatile and fruitful area of research which spans inorganic, organic, biological and materials chemistries (see for example Refs. [1–3]). Since 1991, our research programme has been directed along two broad themes: (i) stoichiometric [4] and catalytic [5] phospho-transfer processes which result in the formation of phosphorus–carbon [P–C] bonds with the generation of new stereogenic centres; and (ii) the ability of chelating poly-organophosphorus(III) ligands to transfer steric and electronic information through the ligand framework and across a metal centre to another ligand (to, for example, a carbonyl ligand) bound to the same metal [6]. We are now extending our earlier work on the latter theme by combining the transfer of stereochemical and configurational information via a phosphorus compound to influence the ability of that compound to discriminate between and interact with substrates of specific configuration. Our strategy towards this goal exploits the well-known ability of functionalised triphenylphosphines to adopt chiral C_3-symmetric propeller-type conformations which minimise intramolecular non-bonded interactions between the stereoelectronically anisotropic phenyl rings. There are many thousands of compounds reported which contain the triphenylphosphine ligand or a derivative thereof. A search

* Corresponding author.

PII S0022-328X(96)06860-X

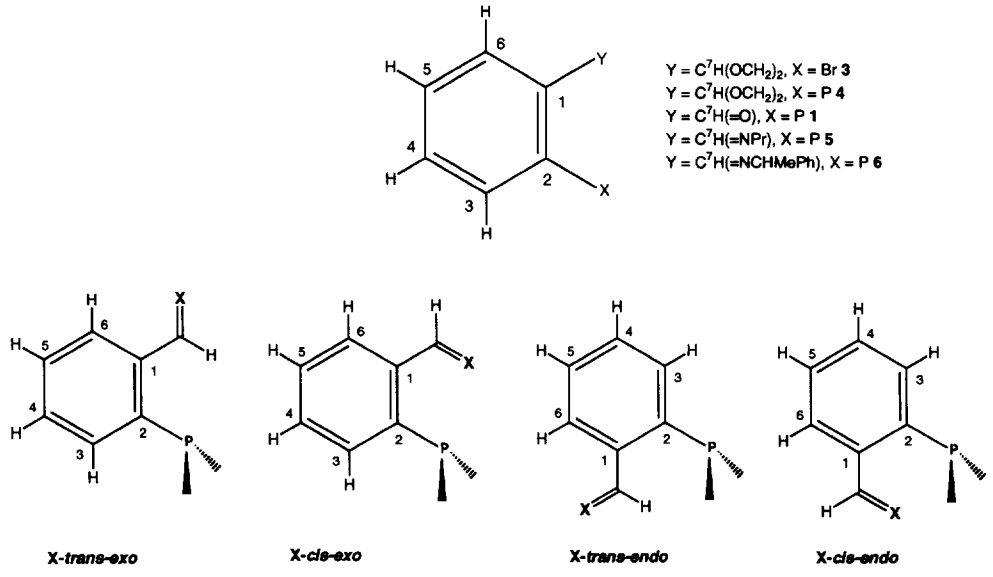

Fig. 1. Labelling scheme and conformational isomers for *tris*-(2-functionalised)triphenylphosphines.

of the Bath Information and Data Services Database using the keywords 'triphenylphosphine' and 'crystal structure' reveals over 600 entries between the years 1981 and 1996. The number of crystal structures containing triphenylphosphine lodged with the CDS Cambridge Structural Database System runs into thousands. For leading references to the phenomenon of triphenylphosphine helicity, see Ref. [7]. Control over the specific configuration of the propeller conformation is facilitated by the incorporation of a stereo-defined function either (a) substituted directly onto the phenyl rings or (b) in the form of a chiral metal complex coordinated to the phosphorus atom. Indeed, the latter strategy has been particularly well investigated and has been shown to result in both structural and chemical differentiation of helical, propeller-like conformations of the PPh_3 phenyl rings [8]. Moreover, it has been demonstrated further that stereochemical information can be transmitted from PPh_3 via a metal atom coordination sphere to control the conformation of a distal organic function [9].

As part of our initial investigations in this field, we needed to select a triphenylphosphine modification strategy commensurate with our intention to examine recognition events where control of helical chirality at phosphorus is key. This required us to address the following two important questions: (i) what types of chiral function would be most desirable in terms of efficiency and flexibility; and (ii) what are the ground-state stabilities and energy barriers to epimerization in such systems and how may they be controlled. This contribution describes our initial investigations.

As our initial system, we have selected to exploit covalently modified triarylphosphines [stereo-definition via method (a) above] in compounds derived from *tris*-(2-carboxaldehyde)triphenylphosphine **1**, first reported in 1973 [10] yet little studied [11] (full spectroscopic studies of **1** and **6** have not previously been reported) over the intervening 20 or so years, in contrast to its close relative 2-diphenylphosphinobenzaldehyde **2**, which has been the subject of several contributions dealing with coordination, organometallic and catalytic chemistry (see for example Refs. [12–14]). Compound **1** has a number of possible conformational isomers connected with the positioning of the carboxaldehyde functions, the most favoured being described with respect to their relationship towards the phosphorus atom (Fig. 1). In addition, each of these carboxaldehyde conformations may exist as a pair of enantiomers due to the canted, C_3-arrangement of the phenyl rings (vide infra). We were especially attracted to the multi-functional framework of **1** since it allows for multi-directional development of molecular interactions controlled by the presence of a suitable binding pin at phosphorus. For example, metal ions should promote *cis-exo* evolution **1a**, whilst an *oxo*-function should promote *trans-exo* **1b** evolution, the two scenarios differing in the spatial dispositions of interaction sites.

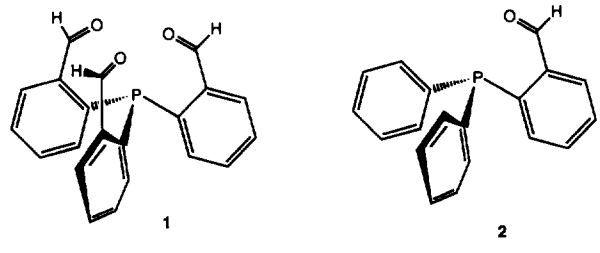

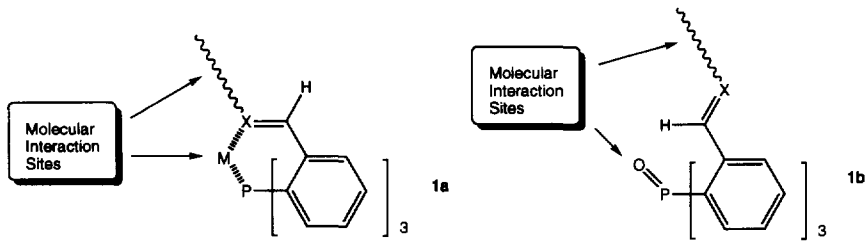

2. Results and discussion

2.1. Synthesis, characterisation and structure of tris-(2-carboxaldehyde)triphenylphosphine 1

The previously published synthesis of **1** is straightforward [10] and, with slight modification, affords *tris*-(2-carboxaldehyde)triphenylphosphine cleanly in three steps as outlined in Scheme 1. Although partial spectroscopic data have been reported for **1**, a full assignment has not previously been published. Since this is of crucial importance to our work, we provide a complete data set for **1** and its derivatives.

The carbonyl group of 2-bromobenzaldehyde is first protected by conversion to the cyclic acetal **3** [10] in 93% overall yield. The four chemically distinct aromatic hydrogens (H3-H6, Fig. 1) appear as multiplets at δ 7.61 (dd), 7.57 (dd), 7.33 (ddd) and 7.21 (ddd) in the ^{1}H NMR spectrum. The dd resonances are obviously associated with H3 and H6 whilst the ddd multiplets are associated with H4 and H5. Similarly, six resonances are observed in the aromatic region of the ^{13}C NMR spectrum. Assignments have been made on the basis of shift correlations and heteronuclear correlation spectroscopy (H-C COSY). In particular, since C1, C3 and C5 should be deshielded by the bromine atom at C2 [15], it is possible to differentiate between C5 and C4 and thus, through analysis of ^{13}C{^{1}H} NMR and H-C COSY spectra, allow complete assignment of ^{1}H and ^{13}C resonances.

Conversion of **3** to the Grignard followed by reaction with the appropriate molar ratio of PCl_3 (THF solvent, -5 °C) affords colourless, crystalline **4** in 77% yield. The ^{1}H and ^{13}C NMR spectra of **4** now contain additional information through coupling to phosphorus which we have found useful in spectroscopic assignment. Thus, four aromatic resonances are observed in the ^{1}H NMR spectrum at δ 7.64, 7.35, 7.23 and 6.87, each resonance being an eight-line doublet of doublet of doublets. The resonances at δ 7.64 and 6.87 may be assigned to either H3 or H6 on the basis of each having only one large $^3J_{HH}$ coupling (H4 and H5 have two large ^3J couplings).

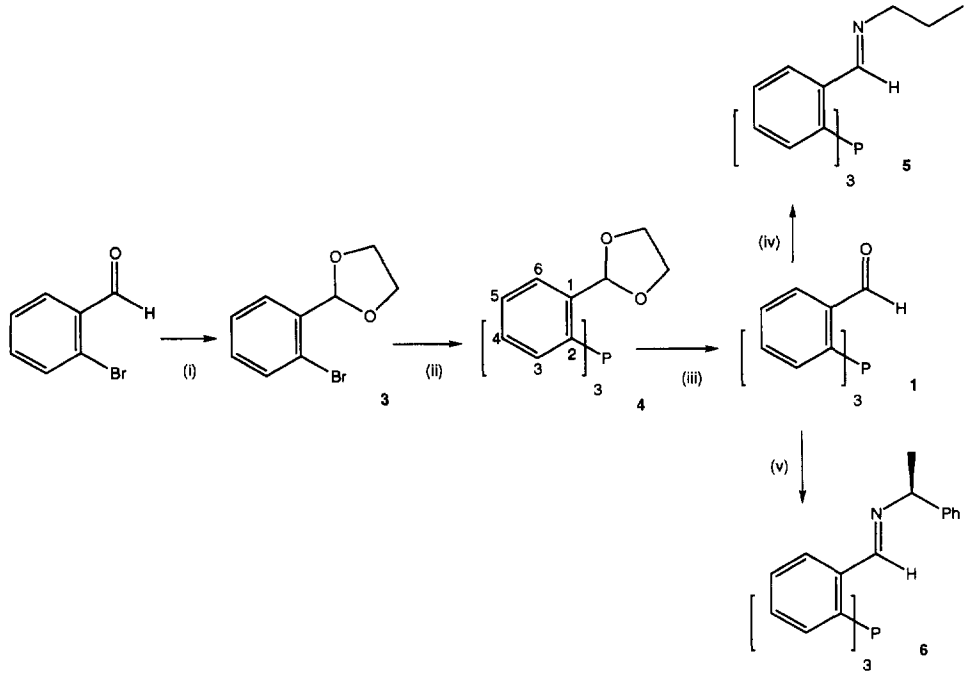

Scheme 1. Synthesis of functionalised triphenylphosphines. (i) $(HOCH_2)_2$, H^+, toluene; (ii) Mg turnings, THF, PCl_3 (1/3 equiv.); (iii) H^+, acetone; (iv) ^{n}PrNH$_2$, CH_2Cl_2; (v) (*S*)-PhCHMeNH$_2$, CH_2Cl_2.

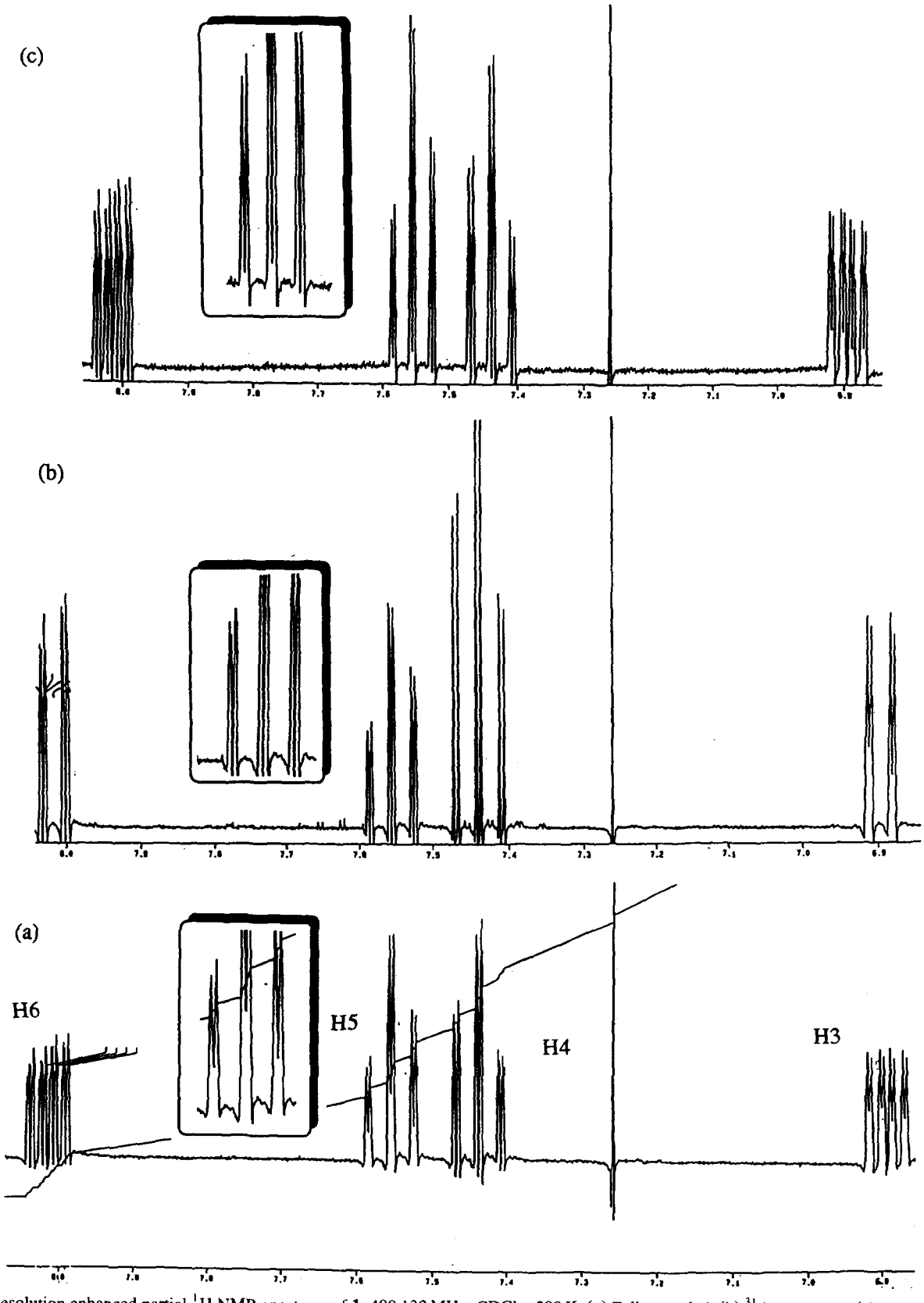

Fig. 2. Resolution enhanced partial ^{1}H NMR spectrum of **1**, 400.132 MHz, $CDCl_3$, 298 K. (a) Fully coupled. (b) ^{31}P decoupled. (c) H7 decoupled. A = H6, B = H5, C = H4 and D = H3 (see Fig. 1 for numbering scheme).

Assignment of H3 to the lower frequency δ 6.87 resonance follows from consideration of the anisotropic shielding effects of the phenyl rings. Specifically, models reveal that rotation around the three [P–C] bonds results in the three H3 hydrogens (one on each phenyl ring) passing over the shielding cone of one of the other phenyl rings (this is shown more clearly below in the crystal structure of *tris*-carboxaldehyde **1**). Hydrogens H6, however, do not pass over similar regions. Consequently, we expect H3 to spend more time in a shielded region than H6 and have a conformationally averaged resonance frequency which is lower than that for H6. Once assignments of H3 and H6 have been made, a complete assignment is facilitated from consideration of the $^{13}C\{^1H\}$ and H-C COSY spectra. These assignments have been confirmed by nuclear Overhauser enhance-

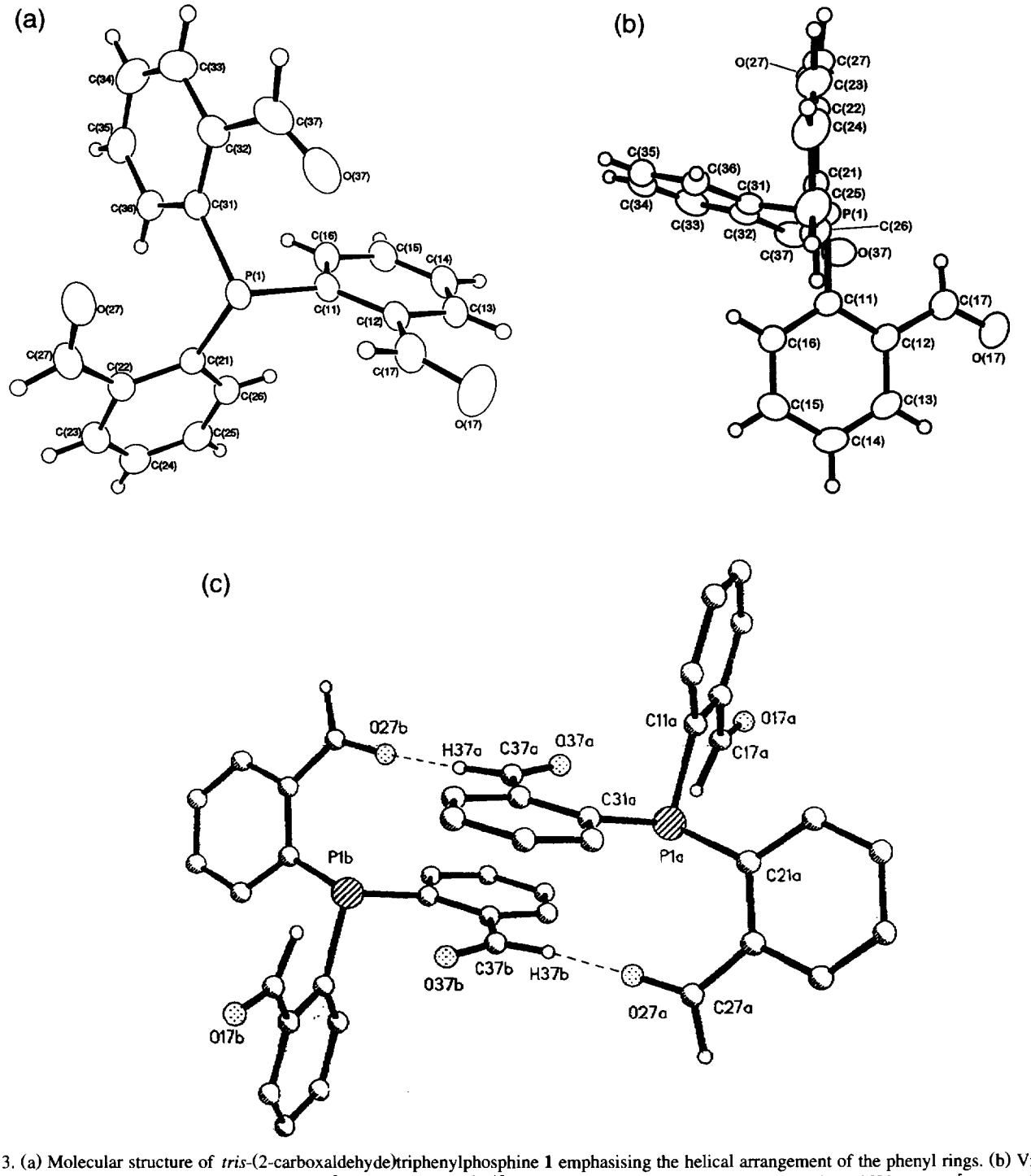

Fig. 3. (a) Molecular structure of *tris*-(2-carboxaldehyde)triphenylphosphine **1** emphasising the helical arrangement of the phenyl rings. (b) View emphasising anisotropic shielding of H3 protons [e.g. attached to C(16)] due to adjacent phenyl rings and deshielding of H6 protons [e.g. attached to C(13)] due to adjacent carboxaldehyde function. (c) Intermolecular hydrogen-bond interactions in **1**.

ment (NOE) experiments on compound **1** described below.

Acid-catalysed hydrolysis of **4** in acetone solvent (which traps the liberated ethan-1,2-diol as the corresponding acetal) affords yellow crystals of **1** in 90% yield [10]. Mass spectrometric and UV spectrophotometric data are fully consistent with the 1,2-disubstituted phenyl substructure [15], and elemental analysis provides compositional data. Full assignments follow from ^{1}H, ^{13}C and H-C COSY spectra along with selective decoupling experiments. A resolution enhanced, fully-coupled partial ^{1}H NMR spectrum of **1** is reproduced in Fig. 2(a). The resonances A (dddd) and D (ddd) are obviously associated with H3 or H6 whilst the multiplets B and C must be assigned to either H4 or H5. Upon phosphorus decoupling (Fig. 2(b)), the signals A, C and D all simplify but that due to B appears as a dddd consistent with that resonance coupling to all four remaining hydrogens. A small coupling of 0.4 Hz was assigned as J_{HH7} on the basis of selective decoupling experiments (Fig. 2(c)). We envisage that this coupling is most likely to be a ^{5}J coupling between H7 and H5 since in this arrangement $^{5}J_{HH}$ coupling is optimised on the basis of the favourable W-arrangement coupling pathway. Moreover, since the corresponding $^{5}J_{HH}$ coupling between H7 and H3, that should be possible in the O-*cis* conformation, is not observed under the same conditions we envisage that the O-*trans* conformer is the more highly populated under these conditions. We are currently probing this problem in more detail and will report our findings in a later contribution [16].

This assignment is also consistent with assigning H3 to the lowest frequency aromatic resonance at δ 6.90 due to a similar conformational shielding effect to that described above for **4**. Indeed, such an explanation provides complete assignments via H-C COSY spectroscopy and is supported by a single-crystal X-ray diffraction study of **1** (see Fig. 3 and Tables 1 and 2 for atomic coordinates and selected interatomic distances and bond angles) which reveals complete rotational averaging at ambient temperature. Fig. 3(b) illustrates how rotation around [P(1)–C(11)] (this being the clearest example) results in H(16) (H3 in Fig. 1) passing adjacent to the shielding zone of the phenyl ring [C(31)–C(36)], whereas H(13) (H6 in Fig. 1) does not. Moreover, as can be seen clearly in the molecular structure of **1** (Fig. 3(b)), the H6 hydrogens (such as that attached to C13 in Fig. 3(b)) are disposed within the deshielding region of the adjacent carboxaldehyde function, consistent with the higher frequency chemical shifts of H6 over H3. Furthermore, were this deshielding scenario the case we would expect H6 for **1** to have a higher frequency than H6 for **4**. Consistently, H6 for **1** appears at δ 8.02 whilst H6 for **4** resonates at δ 7.64. Both of these anisotropic effects lend support to our assignments of H3 and H6 in **1**.

Confirmation of these assignments was provided by NOE experiments on **1**. Low power irradiation of carboxaldehyde hydrogen H7 should result in Overhauser enhancement exclusively to hydrogen H6 (assuming relatively unhindered rotation about C1–C7). As revealed clearly in Fig. 4, irradiation of H7 produces an 11% enhancement (the enhancement being reversible) of the resonance at δ 8.02, that being the only resonance so affected. Consequently, we may be confident in assigning the resonance at δ 8.02 in **1** to H6.

The exploitation of $^{5}J_{HH}$ values for distinguishing between X-*cis* and X-*trans* arrangements (Fig. 1) is well established for substituted benzaldehydes [17] (a $^{5}J_{HH}$ coupling of 0.37 Hz has been reported in benzaldehyde [18]), but should be interpreted with some caution. On the basis of the assignment of **1** made here we conclude that the O-*trans* form is the more favoured in solution, however, we note that in the crystal structure of **1**, two of the three carboxaldehyde groups possess the alternative O-*cis* conformation (Fig. 3(a)). However, this dichotomy is itself not unusual since similar differences between solution and crystal conformations have been reported in 2-diphenylphosphinobenzaldehyde **2**. Indeed, closer examination of the crystallographic data reveals a dimeric structure held together by mutual [C–H · · · O] interactions; within the [C(37)–H(37)–(27)] unit, the [C–O] distance is 3.12 Å with [H–O]

Table 1
Non-hydrogen atomic coordinates ($\times 10^4$) and equivalent isotropic displacement parameters (Å$^2 \times 10^3$) with estimated standard deviations (e.s.d.s) in parentheses

Atom	x	y	z	U_{eq}
P(1)	1841.0(5)	2599.1(3)	−30.0(2)	31.09(13)
C(11)	1762(2)	1899.9(12)	−1022.3(8)	33.8(4)
C(12)	2885(2)	2147.9(13)	−1618.6(9)	36.6(4)
C(13)	2856(2)	1595.5(14)	−2351.3(9)	43.7(4)
C(14)	1730(2)	810.9(14)	−2509.8(10)	46.8(4)
C(15)	596(2)	576.9(14)	−1939.3(10)	45.3(4)
C(16)	614(2)	1115.2(13)	−1203.5(9)	39.9(4)
C(17)	4076(2)	3017.0(15)	−1500.6(10)	47.8(4)
O(17)	5150(2)	3205.7(13)	−1953.9(9)	69.4(4)
C(21)	2509(2)	1498.2(12)	651.5(9)	33.0(3)
C(22)	2806(2)	1705.9(13)	1486.9(9)	36.9(4)
C(23)	3475(2)	914(2)	1984.3(10)	47.8(4)
C(24)	3844(2)	−87(2)	1689.7(10)	50.9(5)
C(25)	3591(2)	−293.1(14)	876.8(10)	47.4(4)
C(26)	2940(2)	489.3(13)	366.8(9)	39.6(4)
C(27)	2476(2)	2740.9(14)	1868.2(10)	44.0(4)
O(27)	1773(2)	3484.4(10)	1550.6(7)	52.2(3)
C(31)	−324(2)	2687.5(12)	158.5(9)	34.5(4)
C(32)	−1242(2)	3515.7(13)	−205.6(9)	41.3(4)
C(33)	−2853(2)	3636(2)	−18.1(12)	54.8(5)
C(34)	−3596(2)	2948(2)	504.2(12)	57.2(5)
C(35)	−2713(2)	2126(2)	853.6(11)	51.3(5)
C(36)	−1103(2)	2004.2(14)	689.7(9)	41.1(4)
C(37)	−577(3)	4277.7(14)	−784.7(11)	52.0(5)
O(37)	741(2)	4219.6(10)	−1073.2(7)	55.2(4)

U_{eq} is defined as 1/3 of the trace of the orthogonalized U_{ij} tensor.

Table 2
Interatomic distances (Å) and angles between interatomic vectors (°) with e.s.d.s in parentheses

P(1)–C(11)	1.840(2)	P(1)–C(21)	1.852(2)	P(1)–C(11)	1.856(2)
C(11)–C(16)	1.395(2)	C(21)–C(26)	1.392(2)	C(31)–C(36)	1.394(2)
C(11)–C(12)	1.408(2)	C(21)–C(22)	1.420(2)	C(31)–C(32)	1.411(2)
C(12)–C(13)	1.392(2)	C(22)–C(23)	1.392(2)	C(32)–C(33)	1.392(3)
C(12)–C(17)	1.479(2)	C(22)–C(27)	1.464(2)	C(32)–C(37)	1.465(3)'
C(13)–C(14)	1.376(3)	C(23)–C(24)	1.377(3)	C(33)–C(34)	1.373(3)
C(14)–C(15)	1.380(3)	C(24)–C(25)	1.378(2)	C(34)–C(35)	1.379(3)
C(15)–C(16)	1.388(2)	C(25)–C(26)	1.390(2)	C(35)–C(36)	1.382(3)
C(17)–O(17)	1.203(2)	C(27)–O(27)	1.209(2)	C(37)–O(37)	1.208(2)
C(31)–P(1)–C(21)	102.91(7)	C(31)–P(1)–C(11)	99.35(7)	C(21)–P(1)–C(11)	101.12(7)
C(16)–C(11)–C(12)	117.83(14)	C(26)–C(21)–C(22)	116.88(14)	C(36)–C(31)–C(32)	117.4(2)
C(16)–C(11)–P(1)	121.92(12)	C(26)–C(21)–P(1)	122.68(11)	C(36)–C(31)–P(1)	122.84(13)
C(12)–C(11)–P(1)	120.26(12)	C(22)–C(21)–P(1)	119.92(11)	C(32)–C(31)–P(1)	119.70(13)
C(13)–C(12)–C(11)	120.1(2)	C(23)–C(22)–C(21)	120.2(2)	C(33)–C(32)–C(31)	120.0(2)
C(13)–C(12)–C(17)	118.3(2)	C(23)–C(22)–C(27)	116.55(14)	C(33)–C(32)–C(37)	117.1(2)
C(11)–C(12)–C(17)	121.54(14)	C(21)–C(22)–C(27)	123.25(14)	C(31)–C(32)–C(37)	122.9(2)
C(14)–C(13)–C(12)	121.0(2)	C(24)–C(23)–C(22)	121.6(2)	C(34)–C(33)–C(32)	121.5(2)
C(13)–C(14)–C(15)	119.6(2)	C(23)–C(24)–C(25)	118.8(2)	C(33)–C(34)–C(35)	118.9(2)
C(14)–C(15)–C(16)	120.1(2)	C(24)–C(25)–C(26)	120.6(2)	C(34)–C(35)–C(36)	120.7(2)
C(15)–C(16)–C(11)	121.3(2)	C(25)–C(26)–C(21)	121.9(2)	C(35)–C(36)–C(31)	121.6(2)
O(17)–C(17)–C(12)	124.6(2)	O(27)–C(27)–C(22)	125.6(2)	O(37)–C(37)–C(32)	125.4(2)

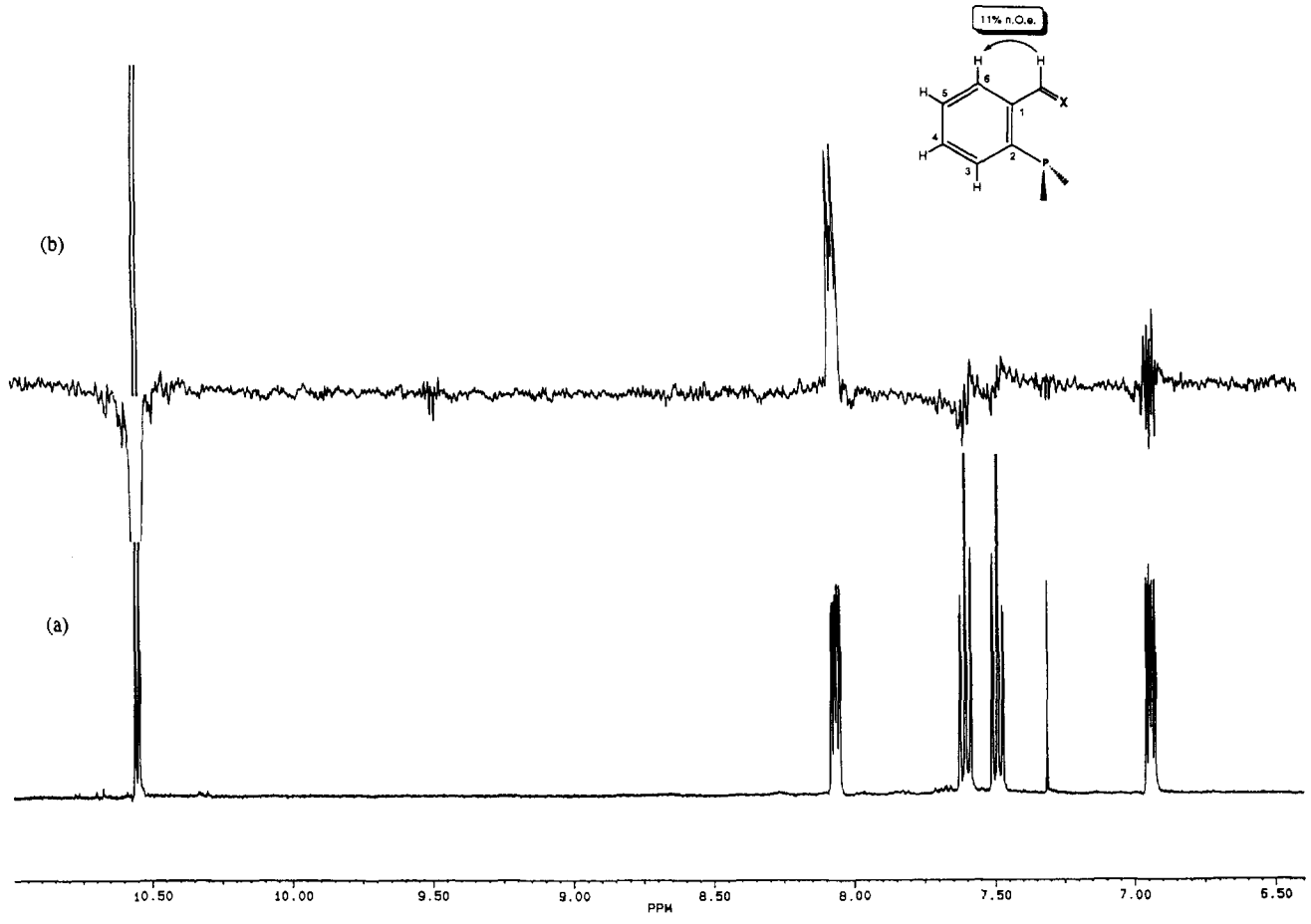

Fig. 4. Nuclear Overhauser enhancement experiment on **1** ($CDCl_3$). (a) Prior to irradiation. (b) Irradiation of H7 resonance at δ 10.56 results in an 11% enhancement at H6 site, δ 8.02.

2.29 Å and a [C–H–O] angle of 154° for normalised positions (Fig. 3(c)). Since the two pairs of carboxaldehyde functions involved in these hydrogen-bonding interactions both possess O-*cis-exo* conformations, it is possible that such interactions may influence the solid state conformations. Their influence over solution phase conformations is less clear although probably far less important under conditions of dilute solution.

2.2. *Schiffs base derivatives of 1: synthesis, characterisation and dynamic behaviour*

Reaction of **1** with $^{n}PrNH_2$ and (*S*)-PhMeCHNH$_2$ (three equivalents) as illustrated in Scheme 1 affords the pale-yellow crystalline *tris*-imine compounds **5** and **6** respectively as reported previously by Brunner and Mokhlesur Rahman [11]. Analytical data and full NMR spectroscopic assignments are provided for both compounds in Section 3, the latter being facilitated by H-C COSY spectroscopy in combination with assignments of H3 and H6 as described above for compounds **4** and **1**.

Given the well-known ability of triphenylphosphine to adopt conformations in which the three phenyl groups orientate themselves in such a manner as to impose an idealised, enantiotopic C_3-symmetry at the phosphorus atom [2], we were interested in ascertaining to what extent such conformational chirality was a feature of compounds **5** and **6**. Ultimately, we envisaged that such chirality may be biased (for example, upon metal ion complexation **1a** or oxygenation at phosphorus **1b**) to promote enantioselectivity in interactions with chiral substrates such as phospho-diesters [3]. A variable temperature ^{1}H NMR experiment (400.132 MHz, C_7D_8) on *tris*-imine **5** between 297 and 223 K revealed no significant changes or decoalesence phenomena in the aromatic and imine resonances. At 193 K, significant broadening of all resonances associated with **5** was observed, consistent with the slowing of intramolecular rotations, but at no time was more than one conformation frozen in which the molecular symmetry was lower than C_3.

However, decoalescence was observed in the central methylene resonance of the propyl group. At 297 K the hydrogens associated with this central methylene resonance appear as the A portion of an $[A_2M_2X_3]$ spin system as a sextet, coupling equally to the two sets of adjacent methylene (M_2) and methyl (X_3) hydrogens. However, at 223 K this signal splits into a more complex nine-line pattern which, on the basis of selective decoupling experiments, is consistent with these two methylene hydrogens becoming diastereotopic and anisochronous (Fig. 5). Unfortunately, the complexity of the two decoalescing multiplets and the small chemical shift differences preclude an accurate determination of exchange rate at coalescence and, with such limited information, it is not possible to conclude the precise

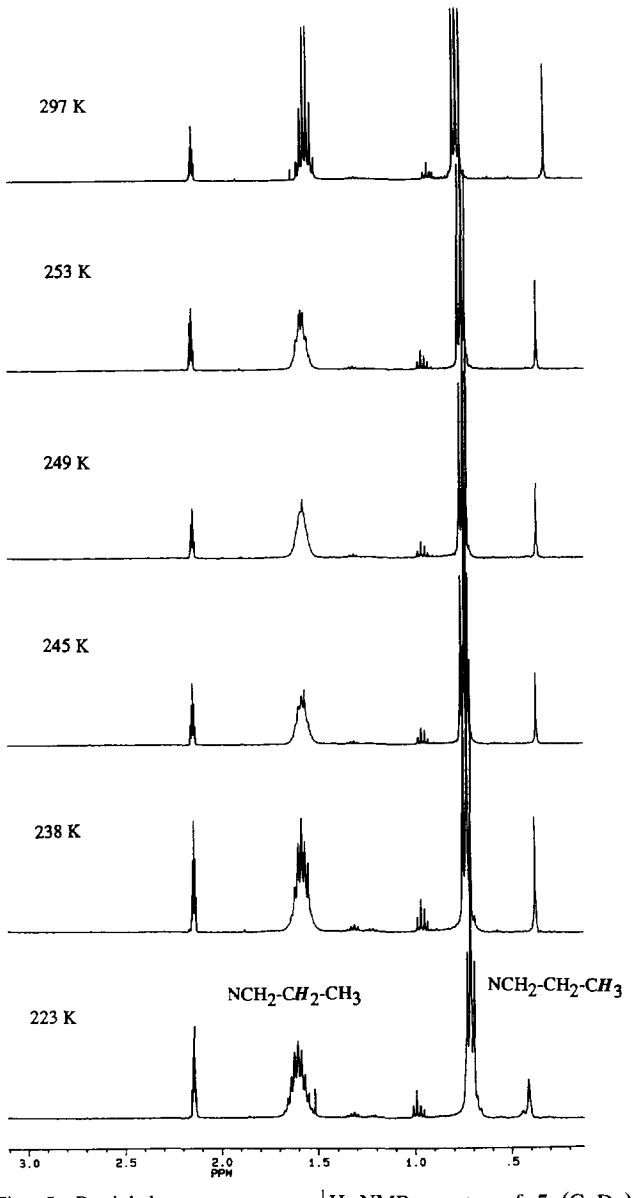

Fig. 5. Partial low temperature ^{1}H NMR spectra of **5** (C_7D_8) showing decoalescence of the resonance attributed to the central n-propyl methylene hydrogens.

nature of this decoalescence phenomenon. However, given the clearly discernable propeller-like arrangement of the phenyl groups in *tris*-carboxaldehyde **1** (Fig. 3(a)), one possibility is the freezing out of an enantiomeric C_3-arrangement with helical chirality. Such a chiral conformer would render adjacent methylene hydrogens diastereotopic. Unfortunately, we were unable to resolve the expected diastereotopicity for the alpha methylene hydrogens.

In an attempt to probe this question of equilibrating chiral conformations further, we reasoned that if a chiral C_3-symmetric propeller-type conformation was accessible in compound **5** then substitution of the achiral propyl function on nitrogen for a chiral substituent, such as the (*S*)-α-methylbenzylamine of compound **6**, would

render the C_3-conformers diastereoisomeric and different sets of signals would be observed for the aromatic and imine hydrogens of **6**. NMR spectroscopy should then be able to distinguish clearly between stereoisomers rather than relying on the generation of diastereotopic hydrogens. Indeed, this proves to be the case; the three chemically equivalent imine hydrogens of **6** afford a clearly resolved doublet resonance (coupling to phosphorus) at δ 8.89 (C_7D_8) at 297 K, but upon cooling to 243(3) K (broadening but unfortunately not decoalescence of the methine C*H*, aromatic hydrogens and ^{31}P resonance is observed over the same temperature range), this resonance decoalesces into two clearly resolved signals in a 53%:47% ratio (the methyl hydrogens also decoalesce in the ratio below 243 K), a ratio which translates to $\Delta G_{eq} = 236(3)\,J\,mol^{-1}$ with an equilibrium constant K of 0.89 at this temperature (Fig. 6).

Analysis of the rate of conformational interconversion between epimer A (major, k_A) and epimer B (minor, k_B) at the coalescence temperature T_C = 263(3) K ($\Delta\nu = 0.038$ ppm, 15.2 Hz by extrapolation) using the method of Shanan-Atidi and Bar-Eli (see Section 3) affords an exchange rate $k = 59\,s^{-1}$ [19–21]. This value compares extremely well with that obtained upon simulation of the individual spectra at temperatures between 301 and 243 K (Fig. 6, see also Section 3), which affords an exchange rate at coalescence of $60\,s^{-1}$. Further spectral simulations also afford exchange rates at 243 K ($k = 0\,s^{-1}$), 253 K ($k = 42\,s^{-1}$),

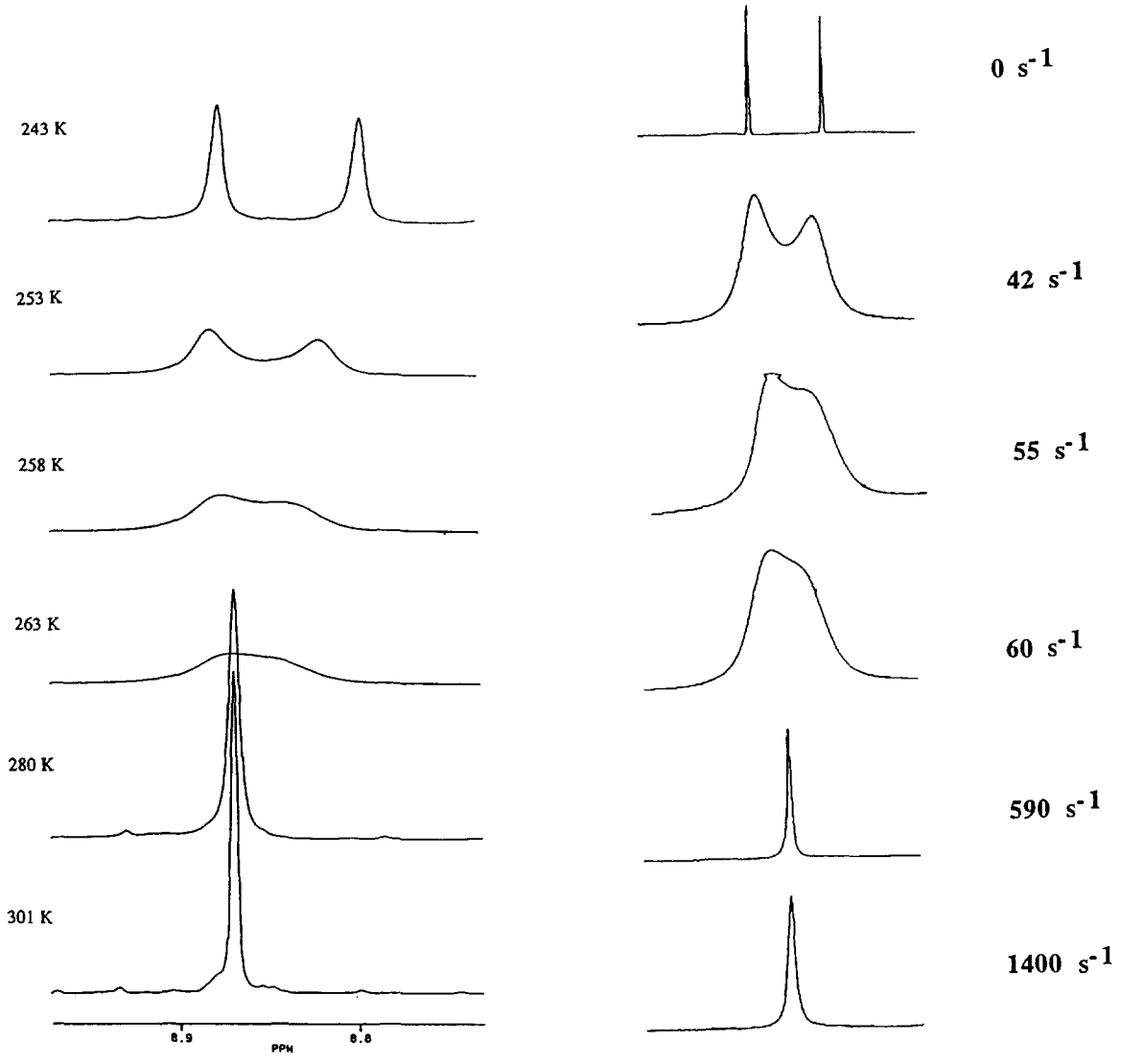

Fig. 6. Partial low temperature ^1H NMR ^{31}P spectrum of **6** (C_7D_8) showing decoalescence of the imine hydrogen resonance due to the freezing of conformational equilibria between diastereoisomers (RHS = calculated; LHS = observed). Exchange rates for the simulated spectra have been computed using the IvorySoft gNMR Simulation Programme.

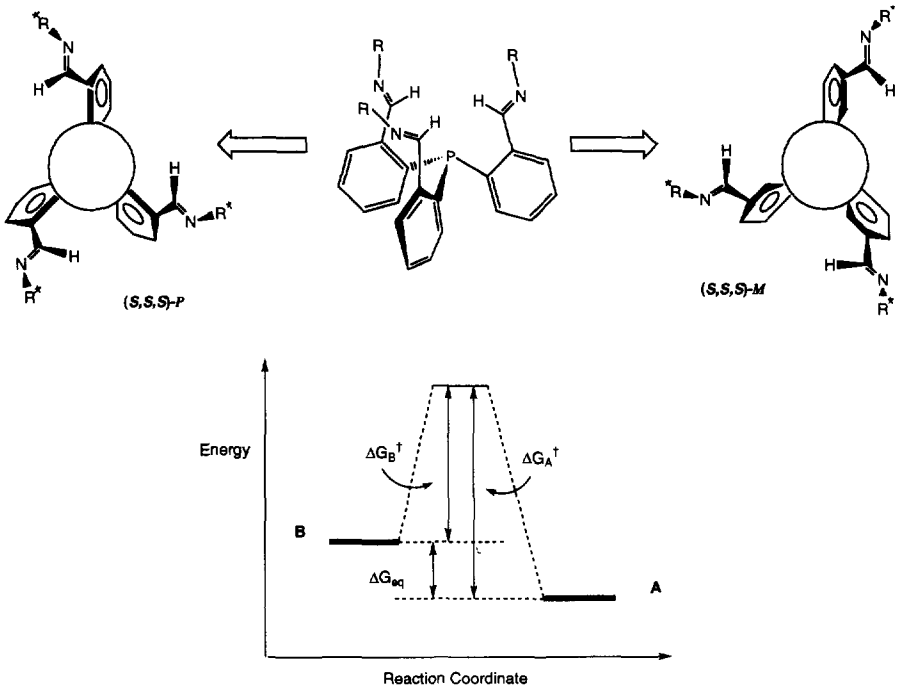

Fig. 7. Representations of possible propeller-type C_3-symmetric conformational epimers for **6**. The stereochemical descriptors for propeller chirality P (plus) and M (minus) follow from work on related systems [22]. Schematic representation (not to scale) of the energy profile for conformational change in **6**; $\Delta G_A^{\dagger} = \Delta G_B^{\dagger}$ ca. 54 kJ mol^{-1} (243 K) and ΔG_{eq}(243) ca. 0.2 kJ mol^{-1}.

258 K ($k = 55\,s^{-1}$), 280 K ($k = 590\,s^{-1}$) and 301 K ($k = 1400\,s^{-1}$). Analysis of these rate data via the Arrhenius equation affords a mean activation energy E_a of 50(2) kJ mol^{-1} [21], whilst analysis via the Eyring equation [21] affords average enthalpy and entropy data of $\Delta H^{\dagger} = 48(2)$ kJ mol^{-1} and $\Delta S^{\dagger} = -25(2)$ J K^{-1} mol^{-1}. Technically, these values are average values since the two epimers involved in the exchange process do not have exactly identical populations and therefore are not degenerate [13]. However, since the free energy difference ΔG_{eq} between epimers at 243 K is only ca. 0.2 kJ mol^{-1} whereas the activation free energy barrier $\Delta G^{\dagger}$ is 54 kJ mol^{-1} at the same temperature, the activation energies for forward and backward processes are essentially equivalent.

It is unlikely that the conformational equilibrium connects N-*cis* and N-*trans* arrangements of the imino function as in Fig. 8, since (i) such behaviour should be observed equally well in both **5** and **6**, resulting in distinct resonances for each imino hydrogen; (ii) the barrier to internal rotation in benzaldehyde is not high enough to prevent rapid rotation at ambient temperature as the ^{1}H NMR spectrum reveals only three multiplets in the aromatic region [18]; (iii) the variable temperature behaviour of both **5** and **6** reveals that each of the imino hydrogens is equivalent in each stereoisomer whereas it would be highly unlikely that all-*cis-exo* or all-*trans-exo* conformations would be the only two observed at low temperature [1], since (iv) ball-and-stick models suggest that the two forms should differ significantly in energy as a result of close contacts between imino substituents being especially acute in the *cis* isomer. This also finds support from solution studies of the conformation preferences in 2-diphenylphosphinobenzaldehyde **2** where the O-*trans* form was found to be the more stable by ca. 3 kJ mol^{-1} [11]. More likely, since analogous decoalescence behaviour is not observed with **5**, the observation of two imine signals in **6** is better attributed to the freezing out of two diastereoisomeric conformations, each of which has an approximate C_3-symmetric environment at phosphorus as proposed above for **5** (Fig. 7).

With this model in hand, we have yet to provide experimental evidence which will illuminate the conformation of the imino groups. Five scenarios are possible: (i) all imines N-*cis-exo*; (ii) all imines N-*trans-exo*; (iii)

[1] We favour the retention of overall C_3-symmetry in these systems since if one of the phenyl substituents had *exo* imine whilst the other two had *endo* groups (or vice versa) then a discrete 2:1 ratio of imino hydrogens would be observed in the low temperature ^{1}H NMR spectra. We further suspect that a C_3 propeller-type conformation is likely to be most energetically favoured on the basis of results from detailed conformational studies on tri-o-thymotide [22]. In this paper, the propeller conformation with the left-handed screw thread is given the descriptor M (for minus) and the right-handed isomer the descriptor P (for plus) and we have adopted the same nomenclature in Fig. 7.

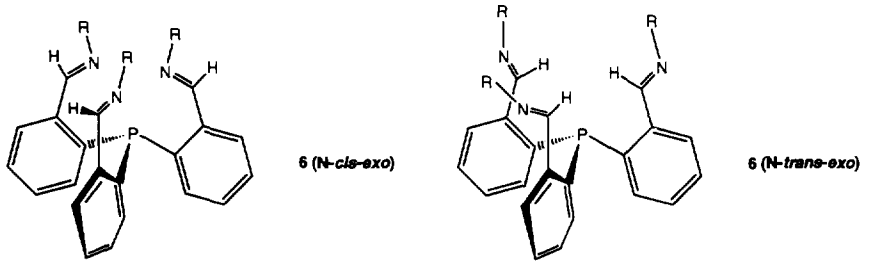

Fig. 8. View emphasising N-*cis-exo* and N-*trans-exo* conformers of *tris*-(2-imino)triphenylphosphines.

all imines N-*cis-endo*; (iv) all imines N-*trans-endo*; or (v) rapid rotation about the $C(sp^2)$–$C(sp^2)$ bond. Molecular models and the structure of *tris*-carboxaldehyde **1** suggest that N-*endo* conformations are significantly less energetically favoured than N-*exo*, effectively eliminating options (iii) and (iv). We envisage that single crystal X-ray diffraction, coupled with variable temperature measurements of $^5J_{H5H7}$ coupling constants, should permit us to address the populations of N-*cis-exo* and N-*trans-exo* conformers (Fig. 8).

A number of studies have previously addressed the problem of conformational equilibria in triphenylphosphine and its derivatives. Torsional angles (θ, Fig. 9) for the phenyl groups have been reported as 22°, 25° and 54° in the crystal [23]. More detailed studies on triphenylphosphine have reported that conformations with C_{3v} point symmetry ($\theta = 0°$, 90°, Fig. 9) are less energetically favourable in solution to those conformers where $\theta = 0°$. Indeed, results from birefringence measurements in benzene solution at 298 K suggest that the most favoured conformers possess $\theta = 59(4)°$ [24] (the corresponding torsional angles θ in **1** are, from the crystal structure, 13.99(4)° (Group 1), 41.76(5)° (Group 2) and 46.03(5)° (Group 3) in which it is the group with the O-*trans-exo* carboxaldehyde function which has the smallest deviation from a vector parallel to the C_3-axis), and it is suggested further that these angles are not altered greatly upon substitution in the *ortho* positions. The crystal structure of **2** [14] reveals that the carboxaldehyde group adopts the O-*cis-exo* conformation as found for two of the carboxaldehyde groups in the crystal of **1**; the third carboxaldehyde function being best described as O-*trans-exo*. Note how the canted arrangement of phenyl rings in **1** allows the molecule to relieve steric pressure between the *ortho*-hydrogens H36, H26 and H16. Furthermore, each carboxaldehyde function is essentially coplanar with its attendant phenyl ring [deviations: 8.23(12)° (Group 1), 8.04(14)° (Group 2), 8.22(11)° (Group 3)] as expected on the basis of attaining optimal conjugation [25].

The energy barrier $\Delta G^{\ddagger}$ for complete rotation around the [P–C_{ipso}] bond of the triphenylphosphine ligand in [(η^5-C_5H_5)Fe(CO)(PPh_3)COMe] [26] has been calculated from variable temperature NMR studies to be ca. 21 kJ mol^{-1} [26] and is a highly facile process which is not frozen out above −90 °C. The mechanism of phenyl ring rotation was found to be complex [26] and proposed to involve a concerted motion of all three phenyls, the lowest energy process involving a 'cog-like' movement of the phenyl rings. However, we have not established that complete rotation about the [P–C_{ipso}] bond is occurring in **6** since it is not a necessary requirement for conformational epimerization in this system. Since complete rotation would require the occupancy of highly sterically-demanding N-*endo* ($\eta = 90°$) conformations, whereas epimerization need not, we envisage that the latter pathway would be the more energetically favoured. However, a number of independent investigations of rotation about an [M–P] bond within a metal–triphenylphosphine complex have been reported to possess simi-

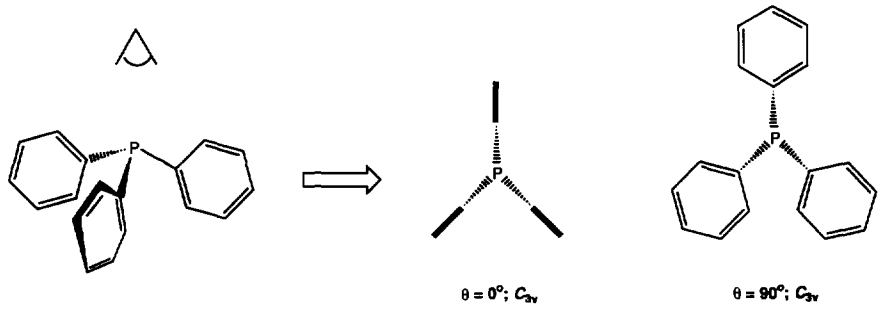

Fig. 9. Perspective view of triphenylphosphine emphasising the torsional angles (θ) for the two high energy C_{3v}-conformations ($\theta = 0°$ and 90°) in triphenylphosphine.

lar energy barriers to that computed for epimerization in **6** ($\Delta H^{\dagger} = 48(2)$ kJ mol^{-1}), for example [(η^5-C_5H_5)Fe(CO)(PPh_3)COMe] with $\Delta H^{\dagger} = 43$ kJ mol^{-1} [26], [(η^5-C_5Me_5)Rh(C_6D_5)[P(C_6H_4Me-4)$_3$]Br] with $\Delta H^{\dagger} = 66$ kJ mol^{-1}, [(η^5-C_5Me_5)Rh[P(C_6H_4Me-4)$_3$]Br_2] with $\Delta H^{\dagger} = 60$ kJ mol^{-1} [27], [(η^6-C_6Me_6)Cr(CO)$_2$(PPh_3)] with $\Delta H^{\dagger} = 28$ kJ mol^{-1} [28]. We suspect that metal chelation to the phosphorus and nitrogen atoms of **6** will raise the energy barrier to epimerization from $\Delta H^{\dagger} = 48(2)$ kJ mol^{-1}.

More closely related studies of conformational preferences in triphenylphosphine and 2-diphenylphosphinobenzaldehyde **2** have been reported, although here the emphasis has been on ground-state effects rather than barriers to conformational change [29,30]. Calculations of relative energies of triphenylphosphine (PPh_3) conformations as a function of torsional angle θ have been performed using both AM1 and STO-3G basis sets, which support energy differences between most and least favoured conformers of ca. 3.5 kJ mol^{-1} [29].

2.3. Conclusion

The observation of conformational diastereoisomerism in a C_3-symmetric system such as **6** [28] raises the interesting possibility of being able to control and increase the levels of diastereoisomerism by manipulating the nature of intramolecular interactions between *ortho*-substituents and the phosphorus centre. For example, binding of the phosphorus and nitrogen donor atoms to a metal ion within a tetrahedral coordination sphere should force the X-*cis*-*exo* conformation (**1a**). Such conformational locking should result in stronger interactions between chiral imino substituents and hence result in greater diastereoselectivities. An alternative strategy would exploit hydrogen-bonding or steric interactions at a phosphorus-bound oxygen atom (**1b**), where now there is a different topology of the interacting sites. With either metal or non-metal atoms playing the role of a chiral pin, conformational locking may then be exploited to promote stereospecific recognition of enantiotopic substrates. Such studies are currently in progress in this laboratory.

3. Experimental details

3.1. General

All reactions and manipulations were performed under inert atmosphere using standard Schlenk, cannula and vacuum techniques unless stated otherwise. Solvents were pre-dried over either sodium wire or calcium chloride prior to reflux and distillation from a suitable drying agent (in parentheses); THF and diethyl ether (sodium benzophenone ketyl), toluene (sodium metal), pentane and dichloromethane (calcium hydride). NMR spectra were obtained on JEOL FX90Q, JEOL FX100, Bruker ARX 250 MHz and AM 400 instruments operating at 100.0 MHz, 250.133 MHz or 400.132 MHz for ^{1}H, 100.614 MHz or 62.895 MHz for ^{13}C and 36.2 MHz or 101.614 MHz for ^{31}P. Deuterated solvents were dried by flash filtration on a column of basic alumina (Brockmann Grade I) and were deoxygenated (dinitrogen purge) before use. All spectra are referenced internally using either the residual solvent resonance for ^{1}H and ^{13}C, TMS as δ_H and $\delta_C = 0$ ppm or the methyl hydrogen resonance of toluene (internal reference) as 2.11 ppm (in C_6D_6 with reference to TMS = 0 ppm). 85% H_3PO_4 was used as external reference for ^{31}P at 0 ppm. All spectra are reported at 298 K unless stated otherwise; the ^{13}C and ^{31}P spectra being run under conditions of broad-band ^{1}H decoupling. Low temperature NMR experiments were performed in either $CDCl_3$ or C_7D_8 solvents. High resolution mass spectrometry was performed by the mass spectrometric service of the School of Chemistry on a VG Autospec instrument operating in the electron impact mode (70 eV). Infrared spectra were recorded on a Perkin-Elmer 457 grating spectrophotometer as Nujol mulls unless noted otherwise. Electronic spectra were recorded on a Perkin-Elmer Lambda 2 spectrophotometer at ambient temperature (ε has units of 1000 cm^2 mol^{-1}). Optical rotations were recorded on an Optical Activity AA 10 polarimeter operating at 589.44 nm at ambient temperature. The compounds PCl_3, NEt_3 and (*S*)-α-phenylethylamine {$[\alpha]^{20}$ −38.9° (neat); lit. −39° Aldrich} were commercial purchases.

3.2. Synthesis of 2-(2-bromophenyl)-1,3-dioxolane 3

A mixture of 2-bromobenzaldehyde (9.99 g, 0.054 mol), ethylene glycol (5.12 g, 0.083 mol) and 4-toluene sulfonic acid (0.46 g, 2.70 mol) in toluene solvent (60 cm^3) was refluxed for 12 h in a vessel fitted with a Dean-Stark condensor. After this time, the mixture was allowed to cool to ambient temperature before being neutralised with saturated aqueous $NaHCO_3$ and washed with saturated aqueous NaCl solution. The toluene extract was then separated, dried over anhydrous Na_2SO_4, filtered and the volatile materials removed under reduced pressure to afford the crude title product. Bulb-to-bulb distillation at 78–80 °C (0.15 mmHg) afforded pure **3** as a colourless liquid (11.53 g, 93%). ^{1}H NMR ($CDCl_3$): δ 7.61 (ddd, 1H, $^5J_{H6H7} = 0.3$ Hz, $^4J_{H6H4} = 1.9$ Hz, $^3J_{H6H5} = 7.7$ Hz, H6); 7.57 (dd, 1H, $^4J_{H3H5} = 1.3$ Hz, $^3J_{H3H4} = 8.0$ Hz, H3); 7.33 (ddd, 1H, $^4J_{H5H3} = 1.3$ Hz, $^3J_{H5H4/6} = 7.6$ Hz, H5); 7.21 (ddd, 1H, $^4J_{H4H6} = 1.9$ Hz, $^3J_{H4H5/3} = 7.7$ Hz, H4); 6.11 (s, 1H, $CH(OCH_2)_2$); 4.09 (m, 4H, $CH(OCH_2)_2$). ^{13}C NMR ($CDCl_3$): δ 136.73 (s, C1); 132.96 (s, C3); 130.97 (s, C4); 127.91 (s, C6); 127.43 (s, C5); 122.96 (s, C2); 102.61 (s, C7); 65.56 (s, C8/9). MS (EI) *m/z*

(relative intensity %): 229 (71, M^+); 185 (35); 169 (8); 156 (17); 149 (45); 73 (100). Anal. Found: C, 46.95; H, 3.80. $C_9H_9O_2Br$ Calc.: C, 47.19; H, 3.96%.

3.3. Synthesis of tris-[2-(1,3-dioxolan-2-yl)phenyl]phosphine 4

A solution of pure 2-(2-bromophenyl)-1,3-dioxolane **3** (11.53 g, 0.05 mol) in THF solution (10 cm^3) was added dropwise over a period of 30 min, via a pressure-equalising, dropping funnel, to a stirred suspension of magnesium turnings (1.31 g, 0.054 mol) in THF (70 cm^3) to which had been added two crystals of iodine. After refluxing for ca. 1 h, the magnesium had been consumed to afford a clear brown solution. The addition funnel was then charged with a solution of PCl_3 (2.31 cm^3, 0.017 mol) in dry THF (30 cm^3) and this solution added dropwise to the Grignard solution, the reaction vessel being maintained at −5 °C by immersion in a rock salt ice-bath. During the course of the addition (ca. 30 min), the initially clear brown reaction solution became yellow and cloudy. Upon complete addition of the PCl_3, the mixture was refluxed for 24 h to afford a clear orange solution. Reaction was then quenched by the addition of saturated aqueous NH_4Cl (50 cm^3) and the crude organic products extracted into toluene (3 × 50 cm^3). Drying over anhydrous Na_2SO_4, filtration and removal of all volatile materials under reduced pressure afforded crude **4**. Pure **4** was obtained as colourless crystals by recrystallisation from toluene–methanol at −35 °C (6.15g, 77%). ^{31}P ($CDCl_3$) −34.31 (s). ^1H NMR ($CDCl_3$): δ 7.64 (ddd, 3H, $^3J_{H6H5}$ = 7.7 Hz, $^4J_{H6H4}$ = 1.4 Hz, $^4J_{H6P}$ = 4.2 Hz, H6); 7.35 (ddd, 3H, $^4J_{H3H5}$ = 1.3 Hz, $^3J_{H5H6/4}$ = 7.5 Hz, H5); 7.23 (ddd, 3H, $^4J_{H4H6}$ = 1.5 Hz, $^3J_{H4H5/3}$ = 7.5 Hz, H4); 6.87 (ddd, 3H, $^4J_{H3H5}$ = 1.3 Hz, $^3J_{H4H3}$ = 7.7 Hz, $^3J_{H3P}$ = 4.4 Hz, H3); 6.30 (d, 3H, $^4J_{H7P}$ = 5.3 Hz, $CH(OCH_2)_2$); 3.95 (m, 12H, $CH(OCH_2)_2$). ^{13}C NMR ($CDCl_3$): δ 142.12 (d, $^1J_{PC2}$ = 21.7 Hz, C2); 135.73 (d, $^2J_{PC1}$ = 17.5 Hz, C1); 134.69 (s, C3); 129.29 (s, C4); 129.04 (s, C5); 126.72 (d, $^3J_{PC6}$ = 5.7 Hz, C6); 101.66 (d, $^3J_{PC7}$ = 25.0 Hz, C7), 65.31 (s, C8/9). MS (EI) *m/z* (relative intensity %): 477 (5, M^+); 449 (100); 405 (80); 333 (98); 261 (85). Anal. Found: C, 67.60; H, 5.60. $C_{27}H_{27}O_6P$ Calc.: C, 67.78; H, 5.69%.

3.4. Synthesis of tris-[2-carboxaldehyde]triphenylphosphine 1

A mixture of *tris*-[2-(1,3-dioxolan-2-yl)phenylphosphine **4** (5.42 g, 0.011 mol) and 4-toluene sulfonic acid (0.48 g, 2.8 mmol) was dissolved in acetone (150 cm^3) and the solution refluxed for 25 h before being allowed to cool to ambient temperature. Water (4 × 20 cm^3) was then added to precipitate the title compound as yellow crystals. Recrystallisation from toluene–pentane at −35 °C afforded pure **1** as yellow–orange crystals (3.52 g, 90%). ^{31}P ($CDCl_3$) −20.8 (s). ^1H NMR ($CDCl_3$): δ 10.56 (d, 3H, $^4J_{H7P}$ = 5.5 Hz, H7); 8.02 (dddd, 3H, $^3J_{H6H5}$ = 7.6 Hz, $^4J_{H6H4}$ = 1.5 Hz, $^5J_{H6H3}$ = 0.5 Hz, $^4J_{H6P}$ = 4.1 Hz, H6); 7.56 (tdd, 3H, $^4J_{H3H5}$ = 1.3 Hz, $^3J_{H5H6/4}$ = 7.5 Hz, $^5J_{H5H7}$ = 0.4 Hz, H5); 7.44 (tdd, 3H, $^4J_{H4H6}$ = 1.6 Hz, $^3J_{H4H5/3}$ = 7.5 Hz, $^4J_{H4P}$ = 0.4 Hz, H4); 6.90 (dddd, 3H, $^4J_{H3H5}$ = 1.3 Hz, $^3J_{H4H3}$ = 7.6 Hz, $^5J_{H3H6}$ = 0.5 Hz, $^3J_{H3P}$ = 4.2 Hz, H3). ^{13}C NMR ($CDCl_3$): δ 191.73 (d, $^3J_{PC7}$ = 18.3 Hz, C7); 139.64 (d, $^1J_{PC2}$ = 25.2 Hz, C2); 138.84 (d, $^2J_{PC1}$ = 16.5 Hz, C1); 134.47 (s, C3); 133.73 (s, C4); 131.84 (d, $^3J_{PC6}$ = 4.7 Hz, C6); 129.40 (s, C5). MS (EI) *m/z* (relative intensity %): 477 (5, M^+); 346 (17); 317 (81); 289 (97); 183 (100). IR (Nujol, KBr, cm^{-1}): 1700 [ν(C=O)]. UV–vis (λ_{max}, $CHCl_3$, nm, $c = 3.7 \times 10^{-5}$ M): 250 [ε_{max} = 20.536, π–π* aromatic K-band], 370 [ε_{max} = 1.082, π–π* aromatic B-band]. Anal. Found: C, 72.80; H, 4.45; M^+ = 346.076 121. $C_{21}H_{15}O_3P$ Calc.: C, 72.83; H, 4.37%; M^+ = 346.075 883.

3.5. Synthesis of tris-(2-propylimino)triphenylphosphine 5

To a solution of *tris*-(2-carboxaldehyde)triphenylphosphine (0.51 g, 1.46 mmol) in CH_2Cl_2 (30 cm^3) was added n-propylamine (0.50 cm^3, 6.08 mmol) and the resulting mixture stirred over Na_2SO_4, under inert atmosphere, for 18 h. After this time the solution was filtered and the volatiles removed to afford a viscous yellow liquid. Dissolution in pentane followed by cooling to −78 °C resulted in crystallisation of the title compound as pale yellow crystals (0.43 g, 62%). ^{31}P ($CDCl_3$) −28.6 (s). ^1H NMR ($CDCl_3$): δ 8.79 (d, 3H, $^4J_{H7P}$ = 5.0 Hz, H7); 7.91 (ddd, 3H, $^3J_{H6H5}$ = 7.6 Hz, $^4J_{H6H4}$ = 1.3 Hz, $^4J_{H6P}$ = 4.2 Hz, H6); 7.31 (td, 3H, $^4J_{H3H5}$ = 1.2 Hz, $^3J_{H5H6/4}$ = 7.5 Hz, H5); 7.17 (td, 3H, $^4J_{H4H6}$ = 1.4 Hz, $^3J_{H4H5/3}$ = 7.5 Hz, H4); 6.80 (ddd, 3H, $^4J_{H3H5}$ = 1.2 Hz, $^3J_{H4H3}$ = 7.7 Hz, $^3J_{H3P}$ = 4.4 Hz, H3); 3.38 (td, 6H, $^3J_{H5H9}$ = 6.8 Hz, $^4J_{H5H10}$ = 0.9 Hz, H8); 1.46 (tsext, 6H, $^3J_{H9H10}$ = 7.1 Hz, H9); 0.67 (t, 9H, $^3J_{H9H10}$ = 7.4 Hz, H10). ^{13}C NMR ($CDCl_3$): δ 159.31 (d, $^3J_{PC7}$ = 21.5 Hz, C7); 139.44 (d, $^1J_{PC2}$ = 18.3 Hz, C2); 136.50 (d, $^2J_{PC1}$ = 16.9 Hz, C1); 134.32 (s, C3); 130.19 (s, C4); 128.93 (s, C5); 127.83 (d, $^3J_{PC6}$ = 4.7 Hz, C6). MS (EI) *m/z* (relative intensity %) 469 (36, M^+); 426 (45); 317 (81); 323 (100). Anal. Found: C, 76.40; H, 7.90; N, 8.70. $C_{30}H_{36}N_3P$ Calc.: C, 76.70; H, 7.70; N, 8.95%.

3.6. Synthesis of tris-{2-[(S)-α-methylbenzyliminol]}triphenylphosphine 6

To a CH_2Cl_2 (50 cm^3) solution of *tris*-(2-carboxaldehyde)triphenylphosphine (1.19 g, 3.44 mmol) was added (*S*)-α-methylbenzylamine (1.38 cm^3, 10.70 mmol)

and the resulting mixture stirred over Na_2SO_4, under inert atmosphere, for 18 h. After this time the solution was filtered and the volatiles removed to afford a viscous yellow liquid which was dissolved in pentane and cooled to −78 °C to afford the title compound as pale yellow crystals (1.10 g, 49%). ^{31}P ($CDCl_3$) −26.2 (s). ^1H NMR ($CDCl_3$): δ 8.86 (d, 3H, $^4J_{H7P}$ = 5.1 Hz, H7); 7.99 (ddd, 3H, $^3J_{H6H5}$ = 7.7 Hz, $^4J_{H6H4}$ = 1.3 Hz, $^4J_{H6P}$ = 4.2 Hz, H6); 7.40 (td, 3H, $^4J_{H3H5}$ = 1.2 Hz, $^3J_{H5H6/4}$ = 7.5 Hz, H5); 7.17 (m, PhH); 6.87 (ddd, 3H, $^4J_{H3H5}$ = 1.2 Hz, $^3J_{H4H3}$ = 7.7 Hz, $^3J_{H3P}$ = 4.4 Hz, H3); 4.38 (q, $^3J_{H8H9}$ = 6.6 Hz, H8); 1.30 (d, 9H, $^3J_{H9H8}$ = 6.6 Hz, H9). ^{13}C NMR ($CDCl_3$): δ 158.10 (d, $^3J_{PC7}$ = 20.3 Hz, C7), 139.46 (d, $^1J_{PC2}$ = 18.3 Hz, C2); 136.95 (d, $^2J_{PC1}$ = 17.8 Hz, C1); 134.49 (s, C3); 130.29 (s, C4); 128.82 (s, C5); 128.31 (s, C6); 128.26 (s, PhC); 126.57 (s, PhC); 69.66 (s, C8); 24.58 (s, CH_3). MS (EI) m/z (relative intensity %): 655 (1, M^+); 550 (100); 105 (79). $[\alpha]_D$ −69.6° (c = 1, $CHCl_3$). UV–vis (λ_{max}, $CHCl_3$, nm, $c = 2.0 \times 10^{-5}$ M): 252 [ε_{max} = 32.432, π–π* aromatic K-band]. Anal. Found: C, 81.95; H, 6.45; N, 6.35; M^+ = 655.310 757. $C_{45}H_{42}N_3P$ Calc.: C, 82.42; H, 6.45; N, 6.41%; M^+ = 655.311 637.

3.7. Variable temperature NMR studies on compound 6

Variable temperature ^1H NMR spectra on **6** were performed on a Bruker AM 400 instrument in C_7D_8 solvent employing broad-band ^{31}P decoupling. Temperatures (±2 K) were taken from a calibrated thermocouple and are uncorrected. Lineshape analysis was performed using the IvorySoft gNMR Simulation Programme. Exchange was studied assuming that the lower exchange limit for the two frozen species had a chemical shift difference (Δδ) of 0.08 ppm (400.132 MHz) at 243 K. This gives results at coalescence which are comparable to those calculated using the method of Shanan-Atidi and Bar-Eli [19]. This is an approximate method of calculating exchange rates at coalescence for those scenarios in which the ratio of the two exchanging species is not 1:1. In the 1:1 case, the rate of exchange (k) at coalescence at T_C is given by the equation $k = \{\pi/[2]^{1/2}\}\Delta\delta$ [21], whereas in the non-1:1 case, Shanan-Atidi and Bar-Eli propose that the appropriate equation to solve is $\Delta P = [(X^2 - 2)/3]^{3/2}1/X$, where ΔP is the fractional polutation difference between exchanging species (in the 1:1 scenario, $P_A = P_B = 0.5$) and $X = 2\pi\tau\Delta\delta$ where τ is the lifetime for exchange and $\Delta\delta$ is the chemical shift difference at coalescence. The exchange rate k is then given by $1/\tau$ and the rate constants for forward and reverse reactions of the exchange pathway are given by $k_A = 2kP_B$ and $k_B = 2kP_A$ respectively [21]. Since $\Delta\delta$ can be obtained by extrapolation and ΔP is calculated readily from the NMR spectrum at zero-exchange, τ is obtained from the standard graph produced by Shanan-Atidi and Bar-Eli [19]. Activation energies were obtained via graphical solution of the Arrhenius expression in the form $\ln k = \ln A - E_a/RT$ (A is the frequency factor and R the gas constant) whilst $\Delta H^\dagger$ and $\Delta S^\dagger$ were obtained via graphical solution of the Eyring equation in the form $\ln k/T = 23.76 + \Delta S^\dagger/8.31 - \Delta H^\dagger/8.31T$ (where T (K) is the temperature).

3.8. Molecular structure determination of 1

All crystallographic measurements were carried out at ambient temperature on a Stoe STADI4 dfffractometer operating in the ω–θ scan mode using graphite monochromated Cu-Kα X-radiation (λ = 1.54184 Å). The data set was corrected for absorption using azimuthal σ-scans (maximum and minimum transmission factors 0.7104 and 0.5664 respectively). The structure was determined by heavy atom methods using SHELXS-86 [32] and was refined by full-matrix least-squares (based on F^2) using SHELXL-93 [33] (Ref. [31]). All data were used in the refinement. Non-hydrogen atoms were refined with anisotropic thermal parameters, hydrogen atoms were constrained to calculated positions (C–H = 0.93 Å) with fixed isotropic thermal parameters of $1.2U_{eq}$ of the parent carbon atoms. The weighting scheme $w = [\sigma^2(F_o^2) + (0.0384P)^2 + 0.5243P]^{-1}$ where $P = (F_o^2 + 2F_c^2)/3$ was used. The final Fourier difference synthesis was flat and showed no features of chemical significance (maximum and minimum residual densities 0.283 and −0.141 e Å^{-3}). Final, non-hydrogen atomic coordinates are given in Table 1. An ORTEX [34] diagram of **1** is given in Fig. 3.

3.8.1. Crystal data

$C_{21}H_{15}O_3P$, 0.46 × 0.345 × 0.23 mm^3, M = 346.3, monoclinic, space group $P2_1/n$, a = 8.3283(4), b = 12.4615(6), c = 16.5132(5) Å, β = 91.314(3)°, U = 1713.34(12) Å^3, Z = 4, D_X = 1.343 Mg m^{-3}, μ = 1.455 mm^{-1}, $F(000)$ = 720.

3.8.2. Data collection

4.0° < 2θ < 50.0°, scan widths 1.05° + α-doublet splitting, scan speeds 1.0–8.0° min^{-1} (subject to a fast pre-scan). Number of data collected 4693, number of unique data n = 2755, number with $F_o > 4.0\sigma(F_o)$ 2528, $R_{int}\{= \Sigma[F_o^2 - F_o^2(\text{mean})]/\Sigma[F_o^2]\}$ = 0.0263, $R_{sig}\{= \Sigma[\sigma F_o^2]/\Sigma[F_o^2]\}$ = 0.0274, T = 200 K.

3.8.3. Structure refinement

Number of parameters p = 364, $R_1\{= \Sigma[F_o - F_c]\}$ = 0.0325, $wR_2\{= (\Sigma[w(F_o^2 - F_c^2)^2]/\Sigma[w(F_o^2)^2])^{1/2}\}$ = 0.0853, goodness of fit$\{= \Sigma[w(F_o^2 - F_c^2)^2]/[(n - p)]^{1/2}\}$ = 1.054, max Δ/δ = 0.001.

Acknowledgements

We are most grateful to the EPSRC for the award of a studentship (to M.R.W.) and for other support of our research programme in phospho-transfer chemistry. K.K.H. thanks Wadham College, Oxford for the award of a Keeley Research Fellowship. Special thanks are extended to (a) Dr. Jonathan Vessey (Leeds) for giving his time and expertise so generously in helping with the variable temperature NMR studies, (b) Dr. Matt Davidson (Durham) for drawing our attention to and delineating the hydrogen-bonded interactions in the crystal structure of **1** and for many enlightening discussions, and also (c) a reviewer for their highly valuable and constructive suggestions. Thanks are due also to Dr. Bernard Watson and Mrs Tanya Marinko-Covell of the University of Leeds Mass Spectrometry Laboratory, Dr. J.M. Brown FRS (Dyson Perrins) for computational facilities and to Professor R. Grigg (Leeds) for access to the polarimeter.

References

[1] C. Yuan and C. Li, *Synthesis*, (1996) 507; W. Huang and C. Yuan, *Synthesis*, (1996) 511; C. Meier and W.H.G. Laux, *Tetrahedron*, *52* (1996) 589; A.B. Smith, K.M. Yager and C.M. Taylor, *J. Am. Chem. Soc.*, *117* (1995) 10879; S.E. Denmark and C-T. Chen, *J. Am. Chem. Soc.*, *117* (1995) 11879; M. Drescher, E Hammerschmidt and H. Kahlig, *Synthesis*, (1995) 1267; N.P. Rath and C.D. Spilling, *Tetrahedron Lett.*, *35* (1994) 227; T. Yokomatsu, T. Yamagishi and S. Shibuya, *Tetrahedron: Asymm.*, *4* (1993) 1779; N.J. Gordon and S.A. Evans, *J. Org. Chem.*, *58* (1993) 5295; R.J. Cross, L.J. Farrugia, P.D. Newman, R.D. Peacock and D. Stirling, *J. Chem. Soc., Dalton Trans.*, (1996) 1637; J. Powell, M.J. Horvath and A. Lough, *J. Chem. Soc., Dalton Trans.*, (1996) 1679; J.M. Harrowfield, M. Mocerino, B.J. Peachey, B.W. Skelton and A.H. White, *J. Chem. Soc., Dalton Trans.*, (1996) 1687; S.L. Bearne and R. Kluger, *Bioorg. Chem.*, *20* (1992) 135; D.M. Coe, S.M. Roberts and R. Storer, *J. Chem. Soc., Perkin Trans. I*, (1992) 2695; H. Mitsuya, R. Yarchoan and S. Broder, *Science*, *249* (1990) 1533. S. Feng and T. Bein, *Nature*, *368* (1994) 834; G. Cao, H-G. Hong and T.E. Mallouk, *Acc. Chem. Res.*, *25* (1992) 420; H.E. Katz, *Science*, *254* (1991) 1485.

[2] M.J. Baker and P.G. Pringle, *J. Chem. Soc., Chem. Commun.*, (1993) 314.

[3] T. Kato, T. Takeuchi and I. Karube, *J. Chem. Soc., Chem. Commun.*, (1996) 953.

[4] P.G. Devitt and T.P. Kee, *Tetrahedron*, *51* (1995) 10987; M.J. Cain, C.A. Baird and T.P. Kee, *Tetrahedron Lett.*, *35* (1994) 8671; V. Sum, C.A. Baird, T.P. Kee and M. Thornton-Pett, *J. Chem. Soc., Perkin Trans. I*, (1994) 3183; P.G. Devitt and T.P. Kee, *J. Chem. Soc., Perkin Trans. I*, (1994) 3169; V. Sum, M. Thornton-Pett and T.P. Kee, *J. Chem. Soc., Chem. Commun.*, (1994) 743; V. Sum and T.P. Kee, *J. Chem. Soc., Perkin Trans. I*, (1993) 1369, 2701; V. Sum, A.J. Davies and T.P. Kee, *J. Chem. Soc., Chem. Commun.*, (1992) 1771.

[5] M.C. Mitchell, A. Cawley and T.P. Kee, *Tetrahedron Lett.*, *36* (1995) 287; P.G. Devitt, M.C. Mitchell, J.M. Weetman, R.J. Taylor and T.P. Kee, *Tetrahedron: Asymm.*, *6* (1995) 2039.

[6] N. Greene and T.P. Kee, *Polyhedron*, *12* (1993) 2471; N. Greene, H. Taylor, T.P. Kee and M. Thornton-Pett, *J. Chem. Soc., Dalton Trans.*, (1993) 821; V. Sum, M. Thornton-Pett and T.P. Kee, *J. Organomet. Chem.*, *438* (1992) 89; V. Sum, M.T. Patel, M. Thornton-Pett and T.P. Kee, *Polyhedron*, *11* (1992) 1743; T.P. Kee and M.T. Patel, *Polyhedron*, *11* (1992) 135; K.M. Cooke, T.P. Kee, A.L. Langton and M. Thornton-Pett, *J. Organomet. Chem.*, *419* (1991) 171.

[7] L.J. Guggenberger, *J. Organomet. Chem.*, *81* (1974) 271; K. Mislow, D. Gust, P. Finocchiaro and R.J. Boettcher, *Top. Curr. Chem.*, *47* (1974) 1; K. Mislow, *Acc. Chem. Res.*, *9* (1976) 26; J. Polowin, S.C. Mackie and M.C. Baird, *Organometallics*, *11* (1992) 3724; S.E. Garner and A.G. Orpen, *J. Chem. Soc., Dalton Trans.*, (1993) 533; H.A. Mayer and W.C. Kaska, *Chem. Rev.*, *94* (1994) 1239.

[8] H. Brunner, R. Oeschey and B. Nuber, *Angew. Chem., Int. Ed. Engl.*, *33* (1994) 866.

[9] G. Palyi, K. Alberts, T. Bartik, R. Boese, G. Frater, T. Herbrich, A. Herfurth, C. Kriebel, A. Sorkanu, C.M. Tschoerner and C. Zucchi, *Organometallics*, *15* (1996) 3253.

[10] G.P. Schiemenz and H. Kaack, *Liebigs Ann. Chem.*, (1973) 1480.

[11] H. Brunner and A.F.M. Mokhlesur Rahman, *Chem. Ber.*, *117* (1984) 710.

[12] T.B. Rauchfuss, *J. Am. Chem. Soc.*, (1979) 1045; *Platinum Met. Rev.*, *24* (1980) 95; D.A. Wrobleski, J.E. Hoots and T.B. Rauchfuss, *Inorg. Synth.*, *21* (1982) 175.

[13] J.C. Jeffery, T.B. Rauchfuss and P.A. Tucker, *Inorg. Chem.*, *19* (1980) 3306.

[14] E.F. Landvatter and T.B. Rauchfuss, *Organometallics*, *1* (1982) 506.

[15] R.M. Silverstein, G.C. Basler and T.C. Morrill, *Spectrometric Identification of Organic Compounds*, Wiley, New York, 4th edn., 1981, Chap. 5.

[16] D.H. Williams and I. Fleming, *Spectroscopic Methods in Organic Chemistry*, McGraw-Hill, New York, 4th edn., 1989, p. 99.

[17] T. Schaefer and C.S. Takeuchi, *Can. J. Chem.*, *68* (1990) 339; R. Laatikainen, K. Tuppurainen, Y. Hiltunen and S. Lotjonen, *Magn. Res. Chem.*, *28* (1992) 1047.

[18] K. Hayamizu and O. Yamamoto, *J. Mol. Spectrosc.*, *28* (1968) 89.

[19] H. Shanan-Atidi and K.H. Bar-Eli, *J. Phys. Chem.*, *74* (1970) 961.

[20] M. Oki, *Applications of Dynamic NMR Spectroscopy to Organic Chemistry*, VCH, Florida, 1985, Chap. 1.

[21] M.L. Martin, J-J. Delpuech and G.J. Martin, *Practical NMR Spectroscopy*, Heydon, London, 1980, Chap. 8.

[22] A.P. Downing, W.D. Ollis and I.O. Sutherland, *J. Chem. Soc. (B)*, (1970) 24.

[23] J.J. Daly, *J. Chem. Soc.*, (1964) 3799.

[24] M.J. Aroney, R.J.W. Le Fevre and J.D. Saxby, *J. Chem. Soc.*, (1963) 1739.

[25] K. Unemoto and K. Ouchi, *Proc. Indian Acad. Sci., Chem. Sci.*, *94* (1985) 1.

[26] S.G. Davies, A.E. Derome and J.P. McNally, *J. Am. Chem. Soc.*, *113* (1991) 2854.

[27] W.D. Jones and F.J. Feher, *Inorg. Chem.*, *23* (1984) 2376.

[28] G. Hunter, T.J.R. Weakley and W. Weissensteiner, *J. Chem. Soc., Dalton Trans.*, (1987) 1545; J.A. Chudek, G. Hunter, R.L. MacKay, P. Kremminger, K. Schlogel and W. Weissensteiner, *J. Chem. Soc., Dalton Trans.*, (1990) 2001.

[29] T. Schaefer, R. Sebastian and F.E. Hruska, *Can. J. Chem.*, *71* (1993) 639.

[30] T. Schaefer, R. Sebastian, R.W. Schrko and F.E. Hruska, *Can. J. Chem.*, *71* (1993) 1384.

[31] B. Bogdanovic, B. Henc, B. Meister, H. Pauling and G. Wilke,

Angew. Chem., Int. Ed. Engl., *11* (1972) 1023; C. Bolm, W.M. Davis, R.L. Halterman and K.B. Sharpless, *Angew. Chem., Int. Ed. Engl.*, *27* (1988) 835; C. Bolm and K.B. Sharpless, *Tetrahedron Lett.*, *29* (1988) 5101; M.J. Burk and R.L. Harlow, *Angew. Chem., Int. Ed. Engl.*, *29* (1990) 1462; H. Adolsson, K. Warnmark and C. Moberg, *J. Chem. Soc., Chem. Commun.*, (1992) 1054; C.J. Tokar, P.B. Kettler and W.B. Tolman, *Organometallics*, *8* (1992) 2737.

[32] G.M. Sheldrick, *Acta Crystallogr., A46* (1990) 467.

[33] G.M. Sheldrick, SHELXL-93, Program for refinement of crystal structures, University of Göttingen, 1993.

[34] P. McArdle, *J. Appl. Cryst.*, *28* (1995) 65.